Substrate Recognition at the Binding Site in Mammalian Pancreatic α-Amylases

Kazuhiko Ishikawa,*,‡ Ikuo Matsui,‡ Shoichi Kobayashi,§ Hiroshi Nakatani,∥ and Koichi Honda‡

National Institute of Bioscience and Human Technology, Tsukuba, Ibaraki 305, Japan, National Food Research Institute, Ministry of Agriculture, Forestry and Fisheries, Tsukuba, Ibaraki 305, Japan, and Department of Food Science and Technology, Faculty of Agriculture, Kyoto University, Sakyo-ku, Kyoto 606, Japan

Received September 4, 1992; Revised Manuscript Received March 16, 1993

ABSTRACT: Porcine and human pancreatic α-amylases (PPA and HPA, respectively) have five binding sites for hexose residues of substrates. As previously reported, when a substrate is too small to occupy subsite 5 of the α-amylases, the optimum pH for catalytic activity changes from neutral to acidic [Ishikawa, K., Matsui, I., Honda, K., & Nakatani, H. (1990) *Biochemistry 29*, 7119–7123]. We studied the mechanism by which the enzyme recognizes the substrate by using the synthetic substrates maltopentaose (G5) and its analogs 4-*O*-α-maltotetraosyl-D-xylose (G4-X), 4-*O*-α-maltotetraosyl-2-deoxy-D-glucose (G4-D), 3-*O*-α-maltotetraosyl-L-sorbose (G4-S), 4-*O*-β-maltotetraosyl-D-glucose (G4β-G), α-maltotetraosyl-β-D-fructose (G4-F), *p*-nitrophenyl α-maltotetraoside (G4-φ), and maltopentaitol (G4-GOH). The reducing-end residues of these substrates, relevant to subsite 5, are D-xylose (X), 2-deoxy-D-glucose (D), L-sorbose (S), D-glucose (G), α-D-fructofuranose (F), *p*-nitrophenyl (φ), and D-sorbitol (GOH), respectively. The optimum pH for catalytic activity on the substrates G5, G4-X, G4-D, G4-S, G4β-G, and G4-φ was neutral, while that for G4-GOH and G4-F was acidic. These results indicate that only six-membered-ring residues and a phenyl group are recognizable by subsite 5. The neutral pH profile for G4-φ suggests that steric compatibility of the substrates at subsite 5 is also important for the enzyme activity. The histidine residue at position 201 is located near subsite 5 and has been shown to be important for substrate recognition in chemical modification studies. Therefore, the catalytic activity of point-mutated HPA (H201N), in which histidine 201 was replaced by asparagine, was examined on the same synthetic substrates. The optimum pH for the mutant H201N HPA was acidic for all the substrates, indicating that subsite 5 of the mutant enzyme did not recognize their reducing-end residues. This indicates that, in addition to steric compatibility, interaction between histidine 201 and the substrate is essential for optimal amylase activity at neutral pH. Furthermore, regulation of the catalytic power and the optimum pH through substrate recognition at subsite 5 was qualitatively explained by an induced-fit effect of a peptide loop containing histidine 201 located at the active site.

We found that the pH for maximal catalytic activity of porcine pancreatic α-amylase (PPA)[1] is acidic, rather than neutral, when the substrate cannot occupy the substrate binding site (subsite 5) of the α-amylase. The optimum pH is 6.9 for starch, amylose, and maltopentaose (G5), but is 5.2 for maltopentaitol (G4-GOH), γ-cyclodextrin, and *p*-nitrophenyl α-D-maltoside (Ishikawa et al., 1990, 1991). Similarly, this substrate-dependent optimum pH was also observed in human pancreatic α-amylase (HPA). Substrate-dependent pH optima might be specific to mammalian α-amylases, since microorganism and plant α-amylases all have acidic optimum pH values, independent of the substrate. The difference between mammalian and microorganism α-amylases in regard to their pH-dependent activity is very interesting in terms of biological evolution, since the amino acid residues comprising their active sites are, in large part, conserved (Svensson, 1988). It is also intriguing in terms of mechanics that the optimum pH shift characteristic of mammalian α-amylases is triggered by the recognition of a substrate at subsite 5 remote from the catalytic site.

We studied the substrate recognition and activity control mechanisms at subsite 5 by using both synthetic substrates and point-mutated enzymes. Maltopentaose analogs with reducing-end terminal residues, other than glucose, were synthesized for use as the substrate for PPA and HPA, and the effects of these different terminal residues upon the activities of the enzymes at different pH levels were examined to determine the structural characteristics of the substrates responsible for the shift in optimum pH relevant to subsite 5. Three histidine residues were suggested to be important for catalysis by chemical modification (Ishikawa & Hirata, 1989) and structural studies (Buisson et al., 1987). An activity assay of three HPA mutants at these three residues indicated that the histidine at position 201 (His201) contributes to substrate recognition at subsite 5. Thus, the H201N HPA mutant, in which His201 was replaced by asparagine, was employed to implicate His201 in the interactions between subsite 5 and the substrates.

MATERIALS AND METHODS

Materials. PPA isozyme I (PPA) was isolated from porcine pancreatin according to the method described previously (Ishikawa & Hirata, 1989). HPA was secreted from yeast

* Author to whom correspondence should be addressed.
‡ National Institute of Bioscience and Human Technology.
§ National Food Research Institute.
∥ Kyoto University.

[1] Abbreviations: porcine pancreatic α-amylase, PPA; human pancreatic α-amylase, HPA; *Bacillus macerans* transglycosylase, BME; D-glucose, G; sucrose, G-F; maltose, G2; maltotriose, G3; maltotetraose, G4; maltopentaose, G5; maltohexaose, G6; cellobiose, Gβ-G; D-sorbitol, GOH; D-xylose, X; L-sorbose, S; 2-deoxy-D-glucose, D; *p*-nitrophenyl, φ; D-fructofuranose, F; 1-*O*-α-methyl-D-glucose, G-M; 4-*O*-α-maltotetraosyl-D-xylose, G4-X; 4-*O*-α-maltotetraosyl-2-deoxy-D-glucose, G4-D; 3-*O*-α-maltotetraosyl-L-sorbose, G4-S; 4-*O*-β-maltotetraosyl-D-glucose, G4β-G; α-maltotetraosyl-β-D-fructose, G4-F; *p*-nitrophenyl α-maltotetraoside, G4-φ; 4-*O*-α-maltotriosyl-1-*O*-α-methyl-D-glucose, G4-M; maltopentaitol, G4-GOH; maltohexaitol, G5-GOH; α-cyclodextrin, α-CD.

0006-2960/93/0432-6259$04.00/0

transformed with a recombinant plasmid that was derived from the original plasmid pAMPA2 (Shiozaki et al., 1990). *Saccharomyces cerevisiae* strain KSC22-1C (*MATa, ssl1, leu2, his3, ura3*) (Suzuki et al., 1989) was used as a recipient strain for the transformation; *ssl1* is a recessive, single-gene mutation causing a supersecretion of lysozyme. A Muta-Gene M13 in vitro mutagenesis kit was purchased from Bio-Rad. Glucoamylase (*Rhizopus niveus*) was purchased from Nacalai Tesque Ltd. *p*-Nitrophenyl α-D-maltotetraoside (G4-φ) was purchased from Calbiochem Co. The MCI GEL column for high-pressure liquid chromatography (HPLC) was purchased from Mitsubishi Kasei Co., Ltd. *Bacillus macerans* transglycosylase (BME) was prepared according to the method of Kobayashi et al. (1978). An enzyme immunoassay kit for HPA (right assay "P-Amylase") was purchased from Sankyo Junyaku Co., Ltd. Bacto-yeast nitrogen base without amino acids was purchased from DIFCO Laboratories. DE52-cellulose resin was purchased from Whatman BioSystems Ltd. Other chemicals were of reagent grade.

Synthesis of Heterooligosaccharides with Glucose Analogs at the Reducing-End Terminal. Heterooligosaccharides tethering L-sorbose (S), D-xylose (X), 2-deoxy-D-glucose (D), sucrose (G-F), cellobiose (Gβ-G), and 1-*O*-α-methyl-D-glucose (G-M) at their reducing-end terminals were synthesized by the transglycosylation reaction of α-cyclodextrin (α-CD) with acceptors (S, X, D, G-F, Gβ-G, and G-M) using BME. One gram of α-CD, 1 g of the acceptor, and 330 Tilden–Hudson units (THUs) (Kitahata et al., 1978) of BME were mixed to make a 100-mL reaction mixture, which was kept at 50 °C, pH 6.0, for 17 h. The solution was then heated in a boiling bath for 10 min to inactivate the BME, and the products were precipitated by adding acetone to a concentration of 90%. The precipitate was then dissolved in a small amount of distilled water, and unreacted α-CD was removed as a precipitate by adding tetrachloroethane (French et al., 1949). Hetero-maltopentaose and hetero-maltotetraose were separated from the effluent and purified using HPLC and an MCI GEL column.

Maltopentaitol (G4-GOH) and maltohexaitol (G5-GOH) were prepared from maltopentaose (G5) and maltohexaose (G6), respectively, by the reductive conversion of their reducing-end glucose into sorbitol (GOH) using sodium borohydride (Walform & Thompson, 1963). The formation of G4-GOH and G5-GOH was confirmed by analyses with paper chromatography (Kitahata et al., 1978; Ishikawa et al., 1990) and reductometry (Dygert et al., 1965). These compounds have no reducing power, although their R_f values are almost the same as those for G5 and G6, respectively.

Figure 1 illustrates the structure of the tethered groups in the synthesized heteromaltopentaoses.

Preparation of Wild-Type and Mutant HPAs. Plasmid YEp-HPASIG, designed to express a pre-HPA gene with a GAL10 promoter (Broach et al., 1983) in yeast, was constructed from the plasmid pAMPA2 (Shiozaki et al., 1990). This plasmid was transformed into yeast according to the method of Kushner (1978), and Leu$^+$ transformants were selected. The transformed yeast cells secreted wild-type HPA when they were cultured in synthetic media containing a 0.67% Bacto-yeast nitrogen base without amino acids, supplemented with a leucine-free amino acid mixture (20–375 μg/mL) (Sherman et al., 1982), sodium phosphate buffer (pH 7.0, 0.1 M), calcium chloride (0.1 mM), and galactose (4%) as a carbon source. Three mutant HPA genes (His101 → Asn, His201 → Asn, and His299 → Asn) were constructed in an M13mp19 vector by site-directed mutagenesis, according to the method

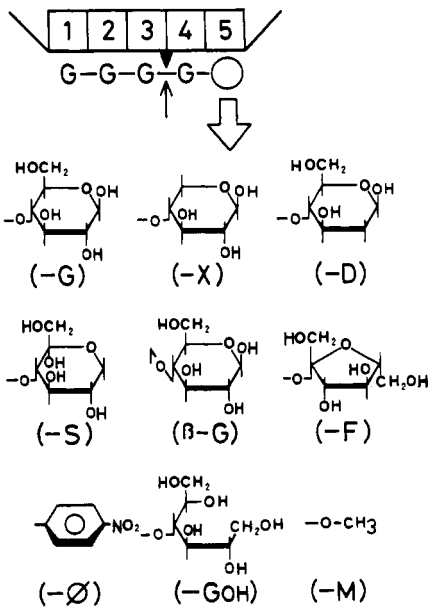

FIGURE 1: Schematic representation of the active site of PPA and HPA, and the significant productive binding mode of the hetero-oligosaccharides (upper figure), and structures of the reducing-end glucose analogs examined (lower figure). Subsites for glucose residues (G) of the substrate are numbered 1–5 from the nonreducing end. The catalytic residues are located between subsites 3 and 4. The substrate in the noticeable productive binding mode is illustrated, where the reducing-end glucose analog (○) is located on subsite 5. Glucose and its analogs are represented as follows: D-glucose, G; D-xylose, X; 2-deoxy-D-glucose, D; L-sorbose, S; D-fructofuranose, F; *p*-nitrophenyl, φ; D-sorbitol, GOH; and methyl residue, M. The α- and β-glucosyl linkages are represented by – and β–.

of Kunkel (1985). The following oligonucleotides were used to create the mutations (bold type and underline denote mutations and codons, respectively):

5′-GTAATTAAT**AAC**ATGTGTGGT-3′
(21-mer; His101[CAT] → Asn; H101N)

5′-GCTTCCAAG**AAC**CATGTGGCCT-3′
(21-mer; His201[CAC] → Asn; H201N)

5′-GTGGATAAC**AAC**GACAATCAA-3′
(21-mer; His299[CAT] → Asn; H299N)

The sequence of the entire coding region of the mutant gene was checked by the dideoxy sequencing method (Sanger et al., 1977).

Purification of Wild-Type and Mutant HPAs. Wild-type HPA was purified from the yeast culture medium according to the method of Matsuura et al. (1978). The culture medium was centrifuged at 6000 rpm for 10 min to remove the yeast. The pH of the supernatant was adjusted to 6.5 with a sodium hydroxide solution, and then solid ammonium sulfate was added to 25% saturation. Corn starch was heated at 70 °C for 30 min in a 15% ammonium sulfate solution, pH 7.8, and was then cooled and added to the reaction solution. The mixture was gently stirred overnight at 4 °C in order to adsorb HPA. The precipitated HPA–starch complex was collected by centrifugation at 4 °C. HPA was liberated from the complex through incubation at 40 °C for 1 h in a solution adjusted to pH 6.5 which contained 0.02 M sodium chloride and 0.01 M calcium acetate. The supernatant solution containing the liberated HPA was dialyzed against 20 mM Tris-HCl buffer (pH 8.3) containing 0.1 mM calcium chloride. The dialyzed solution was chromatographed over DE52-

cellulose, and the HPA was eluted with a sodium chloride gradient (0–0.2 M) of the same buffer.

Mutant HPAs were precipitated with ammonium sulfate added to 75% saturation. The precipitates were dissolved in a phosphate buffer (pH 6.9, 20 mM) containing 0.1 mM calcium chloride and were purified with α-CD-affinity chromatography.

Enzyme Assay and Product Analysis. Catalytic activities of PPA and HPA (wild type and mutant) for the synthetic substrates were assayed as follows. An enzyme reaction was initiated by mixing aliquots of an enzyme solution (1-100 nM) with a substrate solution (0.5-10 mM) of 25 mM Tris–acetate buffer (pH 4.0–9.0) containing 30 mM sodium chloride and 0.1 mM calcium chloride; the reaction was terminated by adding the same volume of 1.0 N sodium hydroxide solution after incubation for an adequate period of time (1–20 min) at 30 °C. Then, the primary products prior to 15% conversion were identified and quantitatively analyzed by HPLC using an MCI GEL column at 65 °C, to determine the initial reaction rate and the hydrolytic patterns of the substrates. In the case of the substrates G4-GOH and G5-GOH, which have no reducing power, reductometric assay (Dygert et al., 1965; Ishikawa et al., 1990) was employed in addition to HPLC analysis, since it is specific and more sensitive to the glucosyl products with reducing power.

The molarities of PPA and HPA were determined to be $A^{1\%} = 24.0\ cm^{-1}$ (Elodi et al., 1972) and $21.0\ cm^{-1}$ (Matsuura et al., 1978), respectively. This determination was made on the basis of the absorbance at 280 nm and their having the same molecular weight (55 000).

RESULTS

Synthesis of Heterooligosaccharides. In order to examine how subsite 5 of the mammalian α-amylase recognizes the different terminal glucose analogs, heterooligosaccharides were prepared by using BME to catalyze the specific formation of an α-1,4 glucosidic bond between the reducing end of the donor and the nonreducing end of the acceptor sugars (Kitahata & Okada, 1975, 1976; Kitahata et al., 1978). Figure 1 lists the following heterooligosaccharides that were made in this way: 4-*O*-α-maltotetraosyl-D-xylose (G4-X), 4-*O*-α-maltotetraosyl-2-deoxy-D-glucose (G4-D), 3-*O*-α-maltotetraosyl-L-sorbose (G4-S), 4-*O*-β-maltotetraosyl-D-glucose (G4β-G), α-maltotetraosyl-β-D-fructose (G4-F), and 4-*O*-α-maltotriosyl-1-*O*-α-methyl-D-glucose (G4-M). About 10-20 mg of the synthetic oligosaccharides (purities > 95%) was isolated by two sequential chromatographic purifications using HPLC, with total yields of no more than 1% [the yield of G4-D was less than 0.3%, owing to the lack of a BME-recognizable hydroxyl group in 2-deoxy-D-glucose (Kitahata et al., 1978)]. The structural integrity of oligosaccharides produced using this method has been verified previously (Kitahata & Okada, 1975, 1976; Kitahata et al., 1978). This structural integrity was further verified by the following identification and stoichiometry of their component sugars resulting from exhaustive hydrolysis with glucoamylase (EC 3.2.1.3; *exo*-1,4-α-D-glucosidase): D-xylose:D-glucose, 1:4, for G4-X; 2-deoxy-D-glucose:D-glucose, 1:4, for G4-D; 3-*O*-α-D-glucosyl-L-sorbose:D-glucose, 1:3, for G4-S; cellobiose:D-glucose, 1:3, for G4β-G; sucrose:D-glucose, 1:3, for G4-F; and 1-*O*-α-methyl-D-glucose:D-glucose, 1:4, for G4-M.

Preparation and Purification of Wild-Type and Mutant HPAs. Yeast transformed with the plasmid pAMPA2, which contains a PH05 promoter and a signal sequence, can secrete HPA (Shiozaki et al., 1990). However, the amount of secreted HPA was insufficient (about 0.4 mg/L), and the induction with low inorganic phosphate medium (Miyanohara et al., 1983) was tedious for such a large-scale culture. Therefore, we constructed the plasmid YEp-HPASIG, which has a strong promoter, GAL10 (Broach et al., 1983), in addition to a signal sequence derived from pAMPA2 (unpublished data). The plasmid was transformed into a supersecretion mutant *S. cerevisiae* strain (KSC22-1C) that expressed a large amount of HPA (2.5 mg/L) in comparison with the original plasmid, pAMPA2. The transformed yeast was cultured at 30 °C for 5 days, and HPA was isolated from the culture medium using the modified method of Matsuura et al. (1978), as described in Materials and Methods. About 1 mg of purified HPA was obtained from 1 L of culture medium. The purified HPA showed a 58-61-kDa component in SDS–PAGE (Figure 2). The difference from the molecular mass (55 kDa) predicted from the amino acid sequence was caused by high mannose-type glycosylation to the protein, since HPA has two potential N-glycosylation sites (Nishide et al., 1986; Sato et al. 1986; Shiozaki et al., 1990). The HPA produced from the yeast showed an activity for G5 almost identical with the HPA purified from human pancreatic juice (Kondo et al., 1990), although their molecular weights are somewhat different. The three mutant HPAs (H101N, H201N, and H299N) were prepared and purified in a similar manner and were also glycosylated. Since both the mutant and the wild-type HPAs cross-reacted with a specific antibody to human pancreatic α-amylase in clinical analysis (Fujisawa et al., 1989), and because their circular dichroism (CD) spectra were identical, the entire three-dimensional structure of the mutant enzymes was considered to be genuine. The wild-type and mutant HPAs were stable in cold, neutral buffer solution for a minimum of several months.

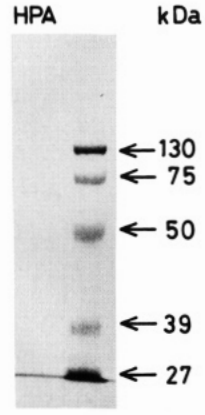

FIGURE 2: SDS–PAGE of purified HPA secreted by yeast. The purified HPA was electrophoresed in a SDS–PAGE gel (15% PA gels with 25 mM Tris–glycine buffer, pH 8.3, containing 0.1% SDS) and stained with Coomassie brilliant blue. The following molecular mass standards were used: phosphorylase *b* (130 kDa), bovine serum albumin (75 kDa), ovalbumin (50 kDa), carbonic anhydrase (39 kDa), soybean trypsin inhibitor (27 kDa), and lysozyme (17 kDa).

Bond Cleavage Pattern for Heterooligosaccharides. The effect of substrate recognition at subsite 5 upon the catalytic activity was analyzed from the bond cleavage patterns of PPA and HPA for a series of synthetic heteromaltopentaoses at pH 6.9. The term "bond cleavage pattern" refers to the distribution of the position and the normalized frequency of bond cleavage in a substrate molecule. Figure 3 shows the cleavage patterns determined by the analysis of the initial digestion products (lower than 15% conversion) catalyzed by PPA and HPA at pH 6.9. The pattern for G5 has been determined by radioactive analysis of the products from ^{14}C-labeled G5 (Ishikawa et al., 1991). Both PPA and HPA

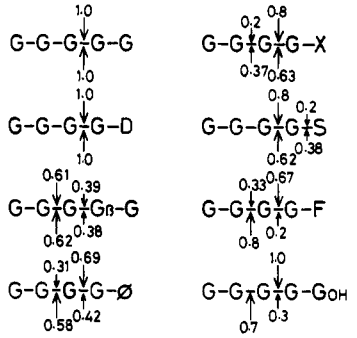

FIGURE 3: Bond cleavage patterns due to the initial action of PPA (upper arros, ↓) and HPA (lower arrows, ↑). The numbers indicated are normalized frequencies at each cleavage position. The reaction was carried out at pH 6.9 and 30 °C. The concentration of the heterooligosaccharides was 7 mM.

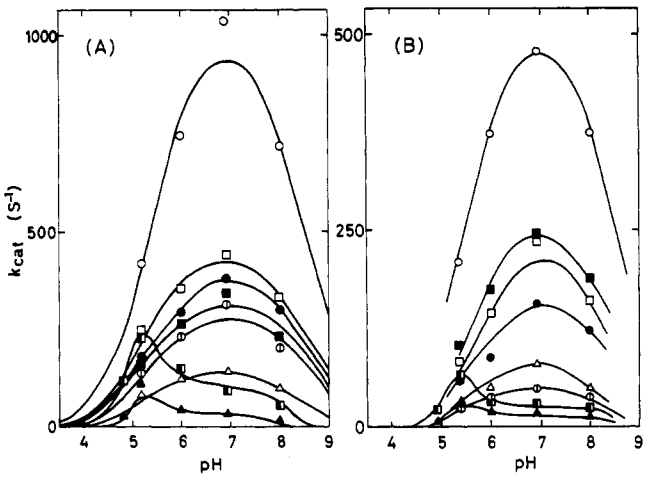

FIGURE 4: pH Profiles of the cleavage activity of PPA (A) and HPA (B) for the heterooligosaccharides. The values of k_{cat} were based on the reaction from the productive binding mode, where the substrate's terminal glucose analog is located on subsite 5, as shown in Figure 1. The reactions were carried out at 30 °C: G5 (○), G4-S (□), G4-X (●); G4-D (■), G4-ϕ (Φ), G4β-G (△), G4-GOH (▣); and G4-F (▲). Solid lines in (A) indicate theoretical curves calculated from eq 1 by using the kinetic parameters (Table II) obtained from the pH profile analysis.

hydrolyzed G5, G4-S, G4-X, G4-D, and G4β-G at the same main cleavage position, although G4β-G showed a different major cleavage site. However, there were different main cleavage positions by PPA and HPA for G4-GOH, G4-F, and G4-ϕ. This is probably due to a subtle difference between the subsite affinities of PPA and HPA for the component residues of the substrates. Hydrolytic activities of HPA and PPA for G4-M were identical with those for G4 (Ishikawa et al., 1991; Robyt & French, 1970), and both substrates were cleaved predominantly at the second glycosidic bond from the reducing end. The methyl group (M) of G4-M was not recognized as a substrate residue by subsite 5 of the α-amylases.

Recognition of Glucose Analogs at Subsite 5. Substrate recognizability (i.e., recognition by subsite 5) was examined by using all of the synthetic substrates, except G4-M. We focused on the cleavage pattern, as shown in Figure 1, where the glucose analog residues bound to subsite 5 and the substrates were cleaved to G3 and a disaccharide comprising glucose and its analog. The pH profiles (plots of the focused cleavage activities of PPA and HPA vs pH) were obtained for all substrates used (Figure 4). The enzymes gave similar pH profiles for each pentamer tested. G5 was the best substrate in the examined pentamer substrates. The optimum pH for a given substrate was also similar between the two enzymes and was dependent on the terminal glucose analog. The results

Table I: Kinetic Parameters of Wild-Type and Mutant HPAs for Amylase Activity[a]

	HPA			
	wild type	H101N	H201N	H299N
k_{cat} (s^{-1})	410 ± 24	3.28 ± 0.10	107 ± 6.7	12.5 ± 0.63
K_m (mM)	0.85 ± 0.15	0.42 ± 0.05	2.75 ± 0.32	0.83 ± 0.13
k_{cat}/K_m (mM^{-1} s^{-1})	482 ± 90	7.8 ± 0.96	39 ± 5.2	15 ± 2.5

[a] Amylase activity was measured in a buffer (20 mM sodium phosphate, pH 6.9) containing 25 mM NaCl at 30 °C, using reductometry with maltohexaitol as a substrate.

indicate that the hydrolysis mechanisms of PPA and HPA are essentially identical, although PPA has a slightly higher activity than HPA for these substrates. This is supported by the fact that they have a high homology (83%) in their primary amino acid sequences and a close resemblance in their active site structures. The pH profiles clearly indicate that subsite 5 can recognize X, S, D, ϕ, and β-G, as well as glucose, for which the optimum pH is 6.9, but for poorly recognized substrates such as F and GOH, the optimum pH shifts to 5.2. For all the substrates, the values of K_m were almost independent of the pH, in the ranges examined, and had values of about 1 mM for G4-X, G4-S, G4-D, G4-F, G4-ϕ, and G4β-G.

Hydrolytic Activity of Mutant HPAs. Previous studies of PPA (Ishikawa & Hirata, 1989; Ishikawa et al., 1991) suggested that there are three histidine residues in the active site, one of which plays an important role in substrate recognition at subsite 5. In the case of HPA, the three histidine residues have proven to be His101, His201, and His299, on the basis of steric structural information on PPA and sequential comparison between PPA and HPA. Thus, we examined the amylase activity of the three mutant HPAs (H101N, H201N, and H299N) to identify the histidine involved in recognition at subsite 5. Asparagine was selected as a substitute for histidine since it cannot be a proton donor or acceptor and its amido group is less bulky than the imidazole ring. The activities of the mutant HPAs were measured for G5-GOH, since this substrate was hydrolyzed efficiently in the same bond cleavage pattern by the wild-type HPA and PPA (Ishikawa et al., 1990). Table I shows the obtained kinetic parameters together with those of the wild-type HPA. The increased K_m value and the slightly decreased k_{cat} value of the H201N HPA strongly suggest that His201 is located at a substrate binding site relatively far from the catalytic site. The drastic decrease in the k_{cat} values of the H101N and H299N HPAs indicates that His101 and His299 play an important role in catalysis, because they exist in or near the catalytic site. Furthermore, the H101N and H299N HPAs exhibited a neutral optimum pH for G5-GOH, as did the wild-type HPA, although their activities were very low, while the H201N HPA showed an acidic optimum pH for the same substrate (Ishikawa et al., 1992). Upon examining the pH profiles of the H201N HPA for the synthesized substrates on the same cleavage patterns as those used to generate Figure 4, we found that its optimum pH was independent of the substrate and was acidic for all substrates examined (Figure 5). The pH profiles of the H101N and H299N HPAs for the synthesized substrates were not observed successfully, since their amylase activities were so small that their transglycosylation activities could not be ignored. However, the above results clearly showed that His201 is located in or near subsite 5 and that interaction between His201 and the substrate is essential for mammalian α-amylases to exert their optimum activity at a neutral pH.

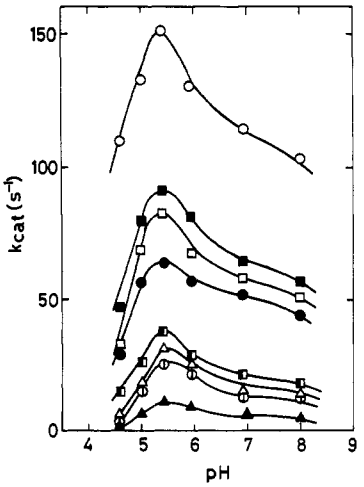

FIGURE 5: pH profiles of the cleavate activity of H201N HPA for the heterooligosaccharides. The values of k_{cat} were based on the reaction from the productive binding mode, where the substrate's terminal analog is located on subsite 5, as shown in Figure 1. The reaction was carried out at 30 °C: G5, (○), G4-S (□), G4-X (●), G4-D (■), G4-ϕ (Φ), G4β-G (△), G4-GOH (◧), and G4-F (▲). Solid lines are not theoretical.

DISCUSSION

Substrate Recognition at Subsite 5. We have shown that subsite 5 of PPA and HPA can recognize the terminal residues of the substrates G5, G4-X, G4-S, G4-D, G4β-G, and G4-ϕ, since the activity optima for all of them are found near neutral pH (Figure 4). A common structural feature of the terminal residues is that they are six-membered-ring molecules. In contrast, the terminal residues F and GOH, which are five-membered and acyclic, respectively, were not clearly recognized by subsite 5, and G4-F and G4-GOH showed an acidic optimum pH. G4-M was excluded from consideration because its bond cleavage pattern was found to be different from those of the other substrates and depended on the concentration of G4-M, as was the case for G4 cleavage by PPA (Robyt & French, 1970). The gradual shift of the optimum pH and the decrease in k_{cat} caused by changes in the terminal substrate glycosyl group suggest that subsite 5 recognizes the overall shape and size of the molecules. This indicates that steric compatibility of the terminal molecule of the substrate is important for recognition at subsite 5. However, it is somewhat strange that the α-G and β-G residues of the substrates G5 and G4β-G, respectively, can both occupy subsite 5, despite their different anomeric linkages. Comparison of the CPK models of these molecules suggests that G4β-G can take a conformation similar to that of G5 when the β-G rotates around the glycosidic bond. Thus, the G4β-G molecule, in the productive binding mode shown in Figure 1, is presumed to have a β-G residue that is rotated appropriately to occupy subsite 5.

Substitution of asparagine for His201 located in subsite 5 of HPA causes the enzyme to exhibit an acidic pH optimum for any substrate examined (Figure 5). This indicates that His201 is essential for substrate recognition at subsite 5, which makes the catalytic function effective near neutral pH. It is unlikely that the mutation (His201 → Asn) induces an enzyme conformation change leading to the change in pH specificity, since the pH profile of the activity for *p*-nitrophenyl maltoside (maltosidase activity) and the hydrolytic pattern for G5-GOH were not influenced by the mutation (Ishikawa et al., 1992). Therefore, subsite 5 of mammalian α-amylases recognizes the substrate not only by the fitness of its size and shape but also through interaction with His201. This interaction may be attributable to the van der Waals forces between the imidazole ring of His201 and the terminal residues of the substrates. A similar interaction was observed in the case of human lysozyme (Muraki et al., 1992).

Scheme I[a]

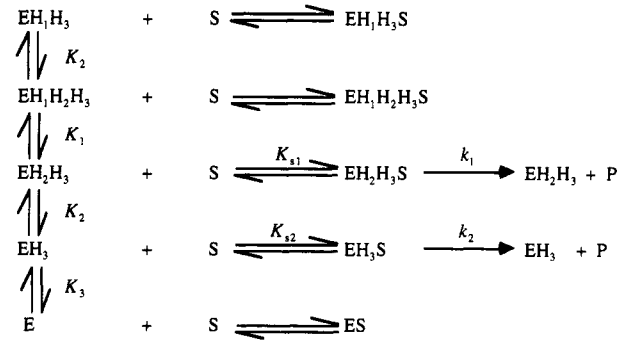

[a] E, S, and P indicate enzyme, substrate, and product, respectively. K_{1-3}, $k_{1,2}$, and $K_{s1,2}$ are the ionization constants for the protons H_{1-3} of the three catalytic residues, the hydrolytic rate constants, and the dissociation constants of the enzyme–substrate complex, respectively.

Table II: Kinetic Parameters Computed from the pH Profiles of PPA[a]

substrate terminal residue	k_1 (s^{-1})	k_2 (s^{-1})
G	342 ± 115	985 ± 84
S	293 ± 46	431 ± 18
X	175 ± 34	387 ± 13
D	187 ± 65	325 ± 26
ϕ	142 ● 66	296 ± 26
β-G	107 ± 12	141 ± 5
GOH	490 ± 37	98 ± 3.8
F	75 ± 8.1	33 ± 5.8

[a] The values of k_1 and k_2 in eq 1 were determined from the pH profile plots using the nonlinear least-squares method and fixed pK_{1-3} values (pK_1 = 4.78; pK_2 = 5.54; pK_3 = 8.62) from a previous study (Ishikawa et al., 1991).

Analysis of pH Profile. In our previous papers (Ishikawa et al., 1990, 1991), we proposed a three-catalytic-residue model based on an analysis of the substrate-dependent shift of the optimum pH for PPA. Since the values of K_m for all the substrates so far examined were independent of pH, the pH dependence of k_{cat} was expressed by eq 1, deduced from the proposed model (Scheme I) (Ishikawa et al., 1991):

$$k_{cat} = \frac{(k_1K_1)/[H^+] + (k_2K_1K_2)/[H^+]^2}{1 + (K_1 + K_2)/[H^+] + (K_1K_2)/[H^+]^2 + (K_1K_2K_3)/[H^+]^3} \quad (1)$$

where $k_{1,2}$ and K_{1-3} denote the rate constants and the ionization constants, respectively, for protons of PPA. Equation 1 is applicable to all substrates by using the previously determined pK_{1-3} values (Ishikawa et al., 1991). The values of k_1 and k_2, which relate to the overall hydrolysis rate, can be determined from an analysis of the pH profiles using eq 1 and a nonlinear least-squares method. Table II lists the kinetic parameters of PPA for the heteromaltopentaosides obtained from the pH profile analysis. Curves calculated from eq 1, using the $k_{1,2}$ values listed in Table II, fit well with experimental data, as shown in Figure 4A. The fact that the values for G4-ϕ are closer to those of G5 than to those of G4-F or G4β-G also indicates that subsite 5 of PPA can recognize a benzene ring more efficiently than it can recognize fructose and β-glucose residues. According to the three-catalytic-residue model, optimum pH should be near neutral when the value of k_1 is

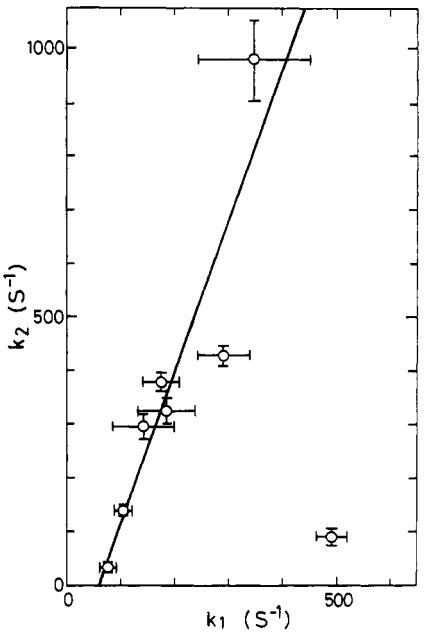

FIGURE 6: Relationship between the rate constants k_1 and k_2 for the catalytic activity of PPA. The solid line is theoretical, calculated from eq 2, using the kinetic parameters listed in Table II. The kinetic parameters for G4-GOH were excluded.

smaller than that of k_2 and should be acidic when k_1 is larger than k_2. Table II and Figure 4A indicate that such a relationship between the kinetic parameters and the optimum pH is valid for the substrates.

As shown in Figure 6, there is a nearly linear relationship between the values of k_1 and k_2, which also holds for all the substrates except maltopentaitol (G4-GOH), which has an acyclic terminal structure. The following linear equation (eq 2) was deduced by the least-squares method:

$$k_2 = a + bk_1 \quad (a = -168 \pm 139;\ b = 2.85 \pm 0.58) \qquad (2)$$

Equation 2 indicates that both k_1 and k_2 values decrease linearly as the pH activity changes from neutrality to acidity. In the ultimate case, where $k_2 = 0\ s^{-1}$, and consequently $k_1 = 58.9\ s^{-1}$ ($= -a/b$), one active enzyme form (EH_3 in Scheme I) becomes completely inactive and the enzyme functions by using only two catalytic residues, as in the case of mold α-amylase (Matsuura et al., 1984). The remarkable deviation of the G4-GOH point from eq 2 suggests a different recognition mechanism of subsite 5 for acyclic residues. This might be supported by the fact that the K_m value for G4-GOH (0.2 mM) (Ishikawa et al., 1990) is considerably smaller than those for the substrates with a cyclic residue (1 mM).

Regulation Mechanism of Mammalian α-Amylase. There are three active histidine residues (His101, His201, and His299) around the catalytic site of PPA, in addition to two catalytic aspartic acid residues (Asp197 and Asp300) (Buisson et al., 1987). Among them, His101 has proven to be the most probable third catalytic residue, since H101N HPA lost amylase activity almost completely. This is consistent with the steric structure that the imidazole ring of His101 is located very near to Asp197 and with our previous identification based on pH profile analysis (Ishikawa et al., 1990, 1991). His201 located near subsite 5 is found to interact with a bound substrate to induce activity that is optimal at neutral pH. His299 may play an important role in catalysis through interaction with the adjacent catalytic residue, Asp300. The binding of a chloride ion to mammalian α-amylases causes an increase in their activities and a shift of their optimum pH to neutrality (Wakim et al, 1969; Levitzki & Steer, 1974). In

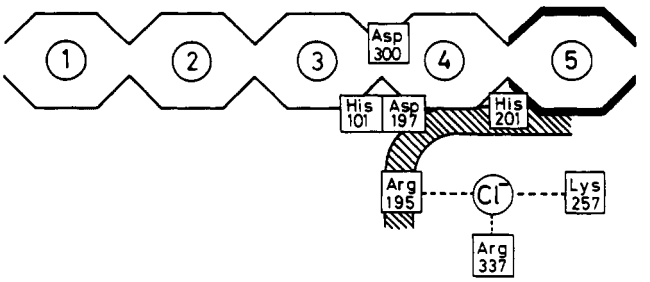

FIGURE 7: Schematic active site model of PPA. Subsites for glucose residues of the substrate are numbered 1–5 from the nonreducing end. The catalytic site is composed of Asp300, Asp197, and His101 and is located between subsites 3 and 4. A chloride ion (Cl^-) is shown binding to Arg195, Lys257, and Arg337. The shaded band along the active site represents a peptide loop containing Arg195, Asp197, and His201.

the case of PPA, the chloride ion binds to Arg195, Lys257, and Arg337 (Buisson et al., 1987). A peptide loop containing Arg195, Asp197, and His201 is located along the catalytic site and could be fixed to the bound chloride ion through Arg195, as well as to the substrate within subsite 5 through His201. The regulation of catalytic function due to the substrate binding to a subsite remote from the catalytic site of the enzyme may be attributable to an induced-fit mechanism (Koshland & Neet, 1968). Figure 7 presents a schematic, mechanistic model showing the correlation of the chloride ion, the subsite, the loop, and the participating amino acids. This model adequately illustrates the effect of the synthesized substrates upon the activity of the mammalian α-amylases. The interaction between His201 and the substrate fitted to subsite 5, in the presence of a chloride ion, induces a subtle configurational change in catalytic residue Asp197 on the loop to activate the neighboring His101. It may also alter Asp300 to change the optimum pH for hydrolytic activity to neutrality. Lack of the loop stabilization by either a chloride ion at Arg195 or a substrate at His201 may result in optimal catalysis that is in an acidic pH region.

The very close sequence homologies among porcine, human, and rat α-amylases suggest that these mammalian α-amylases possess the same general recognition and control mechanisms. Our studies on PPA and HPA provide evidence that the catalytic activity of mammalian α-amylases is controlled by the interaction of the substrate, which is sterically recognized by a binding site, with a key amino acid residue in the same site. The loose substrate recognizability, lacking specific hydrogen bonding, may be physiologically important for allowing mammalian α-amylases to digest modified oligosaccharides in foodstuff in the small intestine (Yoshizawa et al., 1975; Newcomer and McGill, 1966).

ACKNOWLEDGMENT

We wish to thank Dr. K. Shiozaki and Professor K. Matsubara of the Institute for Molecular and Cellular Biology of Osaka University for supplying the plasmid pAMPA2. We are also grateful to Dr. Y. Jigami and his group from the National Institute of Bioscience and Human Technology for helpful discussion.

REFERENCES

Broach, J. R., Li, Y.-Y., Wu, L.-C. Chen, & Jayaram, M. (1983) *Experimental Manipulation of Gene Expression*, pp 82–117, Academic Press, New York.

Buisson, G., Duee, E., Haser, R., & Payan, F. (1987) *EMBO J. 6*, 3909–3916.

Canter, P., & Wells, J. A. (1987) *Science 237*, 394–399.

Dygert, S., Li, L. H., & Thoma, J. A. (1965) *Anal. Biochem. 13*, 367–374.
Elodi, P., Mora, S., & Kryzteva, M. (1972) *Eur. J. Biochem. 24*, 577–582.
French, D., Levine, M. L., Pazur, J. H., & Norberg, E. (1949) *J. Am. Chem. Soc. 71*, 353–356.
Fujisawa, T., Otsuki, M., Okabayashi, Y., Nakamura, T., Fujii, M., Tani, S., Koide, M., Hasegawa, H., & Baba, S. (1989) *Suizo 4*, 31–37.
Ishikawa, K., & Hirata, H. (1989) *Arch. Biochem. Biophys. 272*, 356–363.
Ishikawa, K., Matsui, I., Honda, K., & Nakatani, H. (1990) *Biochemistry 29*, 7119–7123.
Ishikawa, K., Matsui, I., Honda, K., Kobayashi, S., & Nakatani, H. (1991) *Arch. Biochem. Biophys. 289*, 124–129.
Ishikawa, K., Matsui, I., Honda, K., & Nakatani, H. (1992) *Biochem. Biophys. Res. Commun. 183*, 286–291.
Kitahata, S., & Okada, S. (1975) *Agric. Biol. Chem. 39*, 2185–2191.
Kitahata, S., & Okada, S. (1976) *J. Biochem. (Tokyo) 79*, 641–648.
Kitahata, S., Okada, S., & Fukui, T. (1978) *Agric. Biol. Chem. 42*, 2369–2374.
Kobayashi, S., Kainuma, K., & Suzuki, S. (1978) *Carbohydr. Res. 61*, 229–234.
Kondo, H., Nakatani, H., & Hiromi, K. (1990) *Carbohydr. Res. 204*, 207–213.
Koshland, D. E., Jr., & Neet, K. E. (1968) *Annu. Rev. Biochem. 37*, 359–410.
Kunkel, T. A. (1985) *Proc. Natl. Acad. Sci. U.S.A. 82*, 488–492.
Kushner, S. R. (1978) *Genetic Engineering* (Boyer, H. W., & Niscosia, S., Eds.) p 17, Elsevier, Amsterdam.
Levitzki, A., & Steer, M. L. (1974) *Eur. J. Biochem. 41*, 171–180.
Matsuura, K., Ogawa, M., Kosaki, G., Minamiura, N., & Yamamoto, T. (1978) *J. Biochem. (Tokyo) 83*, 329–332.
Matsuura, Y., Kusunoki, M., Harada, W., & Kakudo, M. (1984) *J. Biochem. (Tokyo) 95*, 697–702.
Miyanohara, A., Tho-e, A., Nozaki, C., Hamada, F., Ohtomo, N., & Matsubara, K. (1983) *Proc. Natl. Acad. Sci. U.S.A. 80*, 1-5.
Muraki, M., Harata, K., & Jigami, Y. (1992) *Biochemistry 31*, 9212–9219.
Newcomer, A. D., & McGill, D. B. (1966) *Gastroenterology 51*, 481–488.
Nishide, T., Emi, M., Nakamura, Y., & Matsubara, K. (1986) *Gene 50*, 371–372.
Robyt, J. F., & French, D. (1970) *J. Biol. Chem. 245*, 3917–3927.
Sanger, F., Nicklen, S., & Coulson, A. R. (1977) *Proc. Natl. Acad. Sci. U.S.A. 74*, 5463–5467.
Sato, T., Tsunasawa, S., Nakamura, Y., Emi, M., Sakiyama, F., & Matsubara, K. (1986) *Gene 50*, 247–257.
Sherman, F., Fink, G. R., & Hicks, J. B. (1982) *Methods in Yeast Genetics, A Laboratory Manual*, pp 61–62, Cold Spring Harbor Laboratory Press, Cold Spring Harbor, New York.
Shiozaki, K., Tanaka, K., Omichi, K., Tomita, N., Horii, A., Ogawa, M., & Matsubara, K. (1990) *Gene 89*, 253–258.
Suzuki, K., Ichikawa, K., & Jigami, Y. (1989) *MGG, Mol. Gen. Genet. 219*, 58–64.
Svensson, B. (1988) *FEBS Lett. 230*, 72–76.
Wakim, J., Robinson, M., & Thoma, J. A. (1969) *Carbohydr. Res. 10*, 487–503.
Walform, M. L., & Thompson, A. (1963) *Methods Carbohydr. Chem. 2*, 65–68.
Yoshizawa, S., Moriuchi, S., & Hosoya, N. (1975) *J. Nutr. Sci. Vitaminol. 21*, 31–37.